

## Energy dissipation demand of compression members in concentrically braced frames

Kangmin Lee<sup>†</sup>

*Department of Architectural Engineering, Chungnam National University,  
220 Gung-dong, Yuseong-gu, Daejeon 305-764, Korea*

Michel Bruneau<sup>‡</sup>

*212 Ketter Hall, Department of Civil, Structural, and Environmental Engineering,  
State University of New York at Buffalo, Buffalo, NY 14260, USA*

*(Received December 25, 2003, Accepted April 13, 2005)*

**Abstract.** The response of single story buildings and other case studies are investigated to observe trends in response and to develop a better understanding of the impact of some design parameters on the seismic response of CBF. While it is recognized that many parameters have an influence on the behavior of braced frames, the focus of this study is mostly on quantifying energy dissipation in compression and its effectiveness on seismic performance. Based on dynamic analyses of single story braced frame and case studies, it is found that a bracing member designed with bigger  $R$  and larger  $KL/r$  results in lower normalized cumulative energy, i.e., cumulative compressive energy normalized by the corresponding tensile energy ( $\Sigma E_c/E_T$ ), in both cases.

**Key words:** seismic response; concentrically braced frames; non-linear dynamic analyses; energy dissipation; compression members; slenderness ratios;  $R$  factor.

---

### 1. Introduction

The existing experimental data for bracing members were reviewed by Lee and Bruneau (2002) to assess the extent of hysteretic energy achieved by bracing members in compression in past tests, and the extent of degradation of the compression force upon repeated cycling loading, in an attempt to indirectly quantify their effectiveness and contribution to seismic performance.

In this paper, to expand on this previous study, non-linear dynamic analyses of a single story X-braced bay designed using various  $R$  factors and  $KL/r$  values were conducted to investigate the effect of these parameters on the hysteretic energy dissipation demands on the braces. Hysteretic energy obtained from these non-linear analyses are compared to experimentally obtained capacities, along with other parametric studies. Complementary case studies are also conducted to investigate trends in response and to develop a better understanding of the impact and sensitivity of some design parameters on the seismic response of CBF.

---

<sup>†</sup>Assistant Professor, Corresponding author, E-mail: leekm@cnu.ac.kr

<sup>‡</sup>Professor, E-mail: bruneau@buffalo.edu

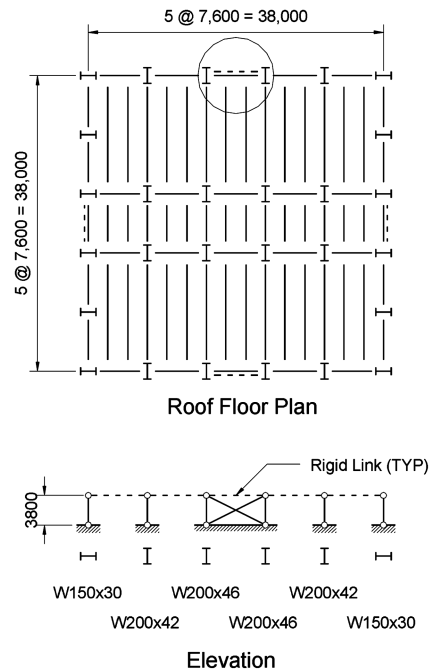


Fig. 1 Building studied (Tremblay and Lacerte 2002)

To make these results broadly and easily accessible to researchers, the complete data from this study, including hysteretic curves from the analyses and all the design outcomes, are provided in the technical report by Lee and Bruneau (2002).

## 2. Non-linear dynamic analyses

### 2.1. Specifics of the building analyzed

The building used for this study is a single story steel building with 38.5 m  $\times$  38.5 m plan dimensions. Lateral bracing is provided by a single braced bay in each exterior frame. As such, this building is identical in geometry to the one designed by Tremblay and Lacerte (2002). The typical floor plan and elevation of this building are shown in Fig. 1. Columns were designed to resist gravity dead and live roof loads of 1.0 kPa and 1.48 kPa respectively. Beams needed not to be designed as the horizontal displacements at the top of columns were constrained to be the same. Braces were designed to resist the seismic loads only. Half of the building floor mass (by tributary area) was assigned to each braced frame to calculate the horizontal seismic design loads. These were calculated in accordance with Uniform Building Code (ICBO, 1994) procedure, specified as:

$$V = C_s W \quad (1)$$

where,  $V$  is the base shear,  $W$  is the total dead load of 1339 kN, and  $C_s$  is the seismic coefficient defined as:

$$C_s = \frac{C_e}{R_w} \quad (2)$$

where,  $R_w$  is the response modification factor (will be discussed in following section) and  $C_e$  is called elastic seismic response coefficient and expressed as:

$$C_e = ZIC \quad (3)$$

where,  $Z$  is the seismic zone factor,  $I$  is the importance factor taken as 1.0, and  $C$  is the numerical constant, defined as:

$$C = \frac{1.25S}{T_1^{2/3}} \quad (4)$$

where,  $S$  is the site coefficient taken as 1.0, and  $T_1$  is the fundamental period of the structure (calculated here from dynamic analyses).

Note that  $Z$  of 0.20 was used here, to match the design by Tremblay and Lacerte (2002) for Vancouver. Also, it is important to realize that based on the procedures described in the following section, the UBC equations only served to give a shape for the elastic design spectra to be divided by  $R$  for brace designs using the AISC LRFD format (and not as suggested by Eq. (2) which would have been applicable for an Allowable Stress Design approach).

## 2.2. Bracing member design

In this paper, bracing members were designed with various slenderness ratios ( $KL/r$ ) and response modification factors ( $R$ ) typically defined as:

$$R = R_d \Omega_0 \quad (5)$$

where  $R_d$  is a reduction factor that accounts for inelastic behavior (a value related to the ductile performance of structural systems) and  $\Omega_0$  is a reduction factor accounting empirically for inherent causes of structural overstrengths that elude accurate calculation. Structural systems with large energy dissipation capacity have large  $R_d$  values and hence are assigned higher  $R$  values, resulting in design for lower forces than systems with relatively limited energy dissipation capacity. The ductility reduction factor,  $R_d$ , is therefore tied to the inelastic characteristics of a structural system, such as energy dissipation and strength degradation. A structural system designed with a high  $R$  value but having a small energy dissipation capacity can fail prematurely when yielding during an earthquake. Therefore, the values of  $R$  have been established considering these factors, coupled with engineering judgment.

Five  $R$  factors were used for design and analysis, namely 1, 2, 4, 6, and 8. Note that an  $R$  factor of 6 is prescribed by the AISC Provisions (AISC, 1997) for SCBF. Three values of brace slenderness ratios were considered, namely 50, 100, and 150 to represent stocky, moderate, and slender braces, respectively. As a result, 15 different bracing members were designed (five  $R$  values times three  $KL/r$  values) and design outcomes are provided in the technical report by Lee and Bruneau (2002).

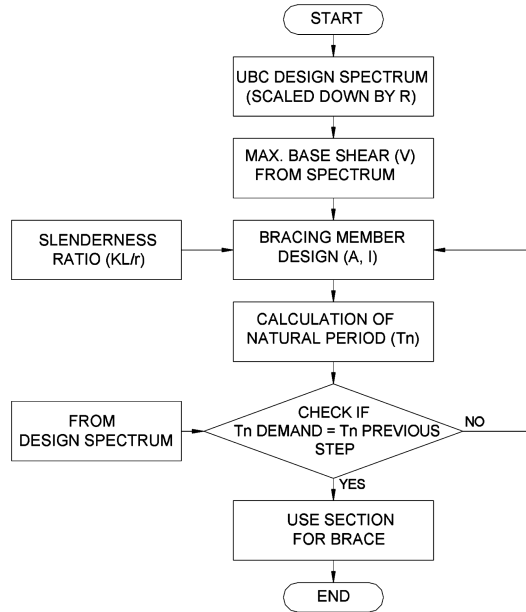


Fig. 2 Bracing member design

**Design Example (R=2, KL/r=50)**

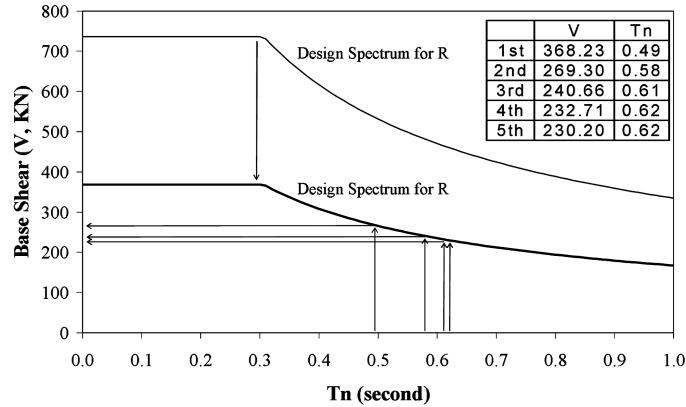


Fig. 3 Design example for braced frame with  $KL/r = 50$  and  $R = 2$

These frames have each been subjected to 6 different earthquake excitations, for a total of 90 non-linear dynamic analyses. Earthquakes used for analyses are summarized in Table 1.

The following design procedure (illustrated in Figs. 2 and 3) was followed to ensure that the resulting strength of each braced frame matched its design spectrum value for the corresponding  $R$  and  $KL/r$  values:

(a) The UBC design spectrum (Fig. 3) was scaled-down by the target  $R$  value.

(b) The maximum specified base shear,  $V$ , from that spectrum (i.e., from the short-period plateau of the spectrum) was considered to initiate the design. Note that both compression and tension brace members in the frame were designed to equally resist base shear,  $V$  (i.e., both compression brace and

Table 1 Bracing members designed

Fundamental period of braced frames, $T$ (seconds)					
$KL/r$	$R=1$	$R=2$	$R=4$	$R=6$	$R=8$
50	0.3489	0.6236	1.0532	1.4196	1.7637
100	0.2621	0.4082	0.6839	0.9285	1.1511
150	0.1748	0.2471	0.3719	0.5038	0.6245
Cross-section area of bracing members, $A$ (mm <sup>2</sup> )					
$KL/r$	$R=1$	$R=2$	$R=4$	$R=6$	$R=8$
50	1037.4	367.7	129.4	70.5	45.9
100	2085.6	858.9	306.5	165.8	108.0
150	4692.7	2346.3	1034.7	564.3	366.7
Plastic section modulus to cross-section area ratio of bracing members, $Z/A$ (mm)					
$KL/r$	$R=1$	$R=2$	$R=4$	$R=6$	$R=8$
50	156.1	156.1	156.1	156.1	156.1
100	78.0	78.0	78.0	78.0	78.0
150	52.0	52.0	52.0	52.0	52.0

tension braces were designed to resist  $V/2$ , respectively).

(c) For the specified design strength and target  $KL/r$  value, the brace area,  $A$ , and inertia,  $I$ , were determined.

(d) The natural period,  $T_n$ , of the resulting braced frame was calculated.

(e) At the calculated period, the required base shear was read from the design spectrum. If this demand was different from the one considered in the previous iteration (or in step (b) for the first iteration), the new specified base shear was therefore considered in step (c) to redesign the brace. If the demand was identical to the one considered, the iteration processed ended.

Square Hollow Structural Sections (HSS), also known as tubes, were selected for all designs, as this was apparently the structural section type that was apparently the most frequently tested (Lee and Bruneau 2002). Note that member sizes (i.e., width and thickness of the square tubular sections with various  $b/t$  ratios) were selected to provide a strength that perfectly matched the brace forces resulting from the loads applied to the braced frames. These were calculated using the, solver function in a spreadsheet program. The corresponding braces are therefore “virtual members” that have the desired properties but that may not correspond to an available shape listed in the AISC Manual (AISC, 1993). The resulting bracing member characteristics obtained from following above procedures are summarized in Table 1, described in terms of cross sectional area of bracing members,  $A$ , period of braced frames,  $T$ , and plastic modulus to cross sectional area of bracing members,  $Z/A$ . The complete set of brace force-displacement hysteretic loops for various  $KL/r$  and  $R$  factors obtained from these analyses are provided in the technical report by Lee and Bruneau (2002).

### 2.3. Brace models considered

Analytical models to represent the cyclic behavior of steel bracing members have been developed by many researchers. These models simulate several important phenomena observed during the inelastic

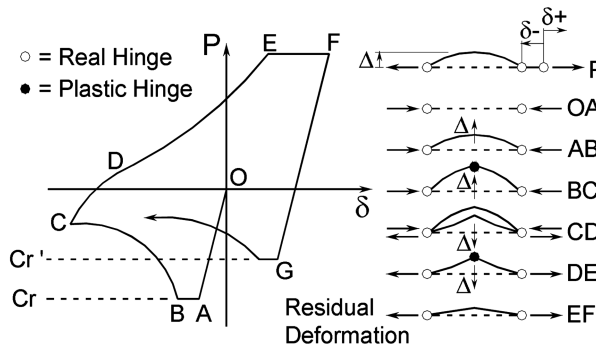


Fig. 4 Zone definitions of refined physical theory model (Bruneau *et al.* 1998)

cyclic loading of braces, such as progressive deterioration of the compression buckling strength, and residual elongation due to plasticity. Analytical models for steel bracing members can be classified into three general types, namely: (a) finite element models; (b) phenomenological (empirical) models, and; (c) physical models.

Phenomenological models of the cyclic behavior of braces have been developed and refined by Jain *et al.* (1977), Ikeda *et al.* (1984), Lee and Goel (1987), and Hassan and Goel (1991). These models are based on simplified empirical rules which can mimic the observed axial force-axial displacement hysteretic curves of the bracing members.

Brace models based entirely on physical behavior (physical brace models) were developed by Nonaka (1987), Gugerli and Goel (1982), and Ikeda and Mahin (1984) to simulate the cyclic buckling behavior of steel braces. Taddei (1995) implemented the Ikeda and Mahin model in Drain-2DX. This model is based on an analytical expression of the axial force ( $P$ ) versus axial displacement ( $\delta$ ), describing the behavior of steel brace members. The model divides a hysteretic cycle into six possible zones of behavior, over which simple formulations are used to approximate the physical characteristics. Fig. 4 shows the zones of physical behavior.

In this paper, the refined physical model was used for non-linear dynamic analysis. Though this model requires more computation time than the phenomenological model, it was deemed to capture more accurately the cyclic inelastic behavior of bracing members.

Table 2 Earthquake records used

Event	Station	Comp.	Scaled			Scale Factor
			PHA (mm/s <sup>2</sup> )	PHA (g)	PHV (mm/s)	
1940 Imperial valey, Ca	El Centro	S00E	2406.8	0.25	3.3	0.70
1971 San Fernando, Ca	Hollywood Storage, L.A.	N90E	1962.8	0.20	2.1	0.95
1971 San Fernando, Ca	Hollywood Storage, L.A.	S00W	2282.9	0.23	1.7	1.36
1949 Western Washington, Wa	Olympia, Highway Test lab.	N04W	1598.1	0.16	2.1	0.99
1983 Coalinga Aftershock, Ca	Oil Fields Fire Station	N270	2538.6	0.26	1.6	1.20
Simulated Motion, Mw=7.2 R=70 km		-	2271.4	0.23	1.9	2.12

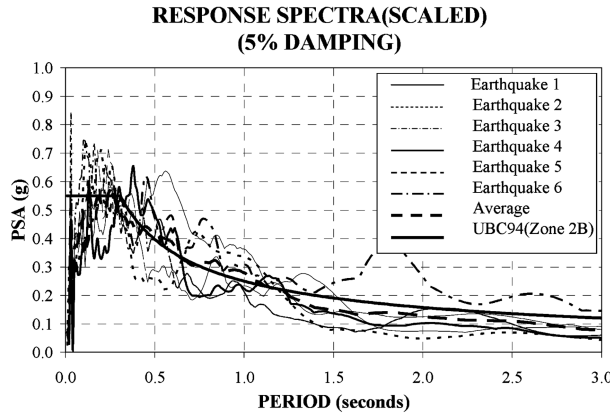


Fig. 5 Scaled response spectra

#### 2.4. Non-linear dynamic analyses

Six ground motions were used in the non-linear dynamic analyses (Table 2). With these ground motions, response spectra with 5% damping were constructed and scaled to match the UBC 94 Zone 2B spectra as much as possible over the range of periods from 0 to 3, using least square method. The scaled response spectra are shown in Fig. 5.

All non-linear dynamic analyses have been performed using Drain-2DX (1993), and the Ikeda and Mahin physical brace (element No. 5) implemented in Drain-2DX by Taddei (1995).  $P-\delta$  effects were included in analyses, and 5% damping was used.

### 3. Normalized cumulative energy demands ( $\Sigma E_C/E_T$ )

Results from the non-linear dynamic analyses conducted in the previous section are investigated and correlated with the existing experimental data reviewed by Lee and Bruneau (2002). In particular, the

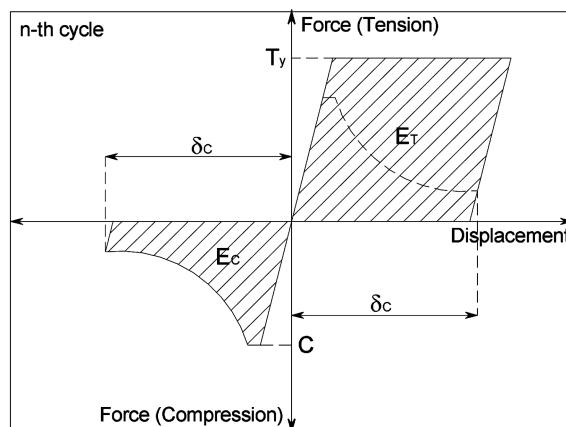


Fig. 6 Definition of dissipated energy ratio,  $E_C/E_T$  (Lee and Bruneau 2002)

Table 3  $\Sigma E_C/E_T$  from experimental data (Lee and Bruneau 2002)

Exp. Data	$KL/r = 50$ (0 - 75)	$KL/r = 100$ (75 - 125)	$KL/r = 150$ (125 - 200)
Avg.	3.79	2.56	2.28
Max.	8.22	6.11	2.28
Min.	1.70	0.72	2.28

Table 4  $\Sigma E_C/E_T$ , story drift, and ductility demands from analysis results

Normalized cumulative energy, $\Sigma E_C/E_T$																
Analysis Results	$KL/r = 50$					$KL/r = 100$					$KL/r = 150$					
	$R=$	1	2	4	6	8	1	2	4	6	8	1	2	4	6	8
Avg.	0.0	3.9	3.8	3.2	2.7	0.0	3.1	2.5	2.0	1.6	0.0	0.0	2.5	1.7	1.6	
Max.	0.0	7.7	6.1	5.7	4.5	0.0	6.2	4.6	3.7	3.2	0.0	0.0	3.7	3.6	3.1	
Min.	0.0	1.2	1.8	1.5	1.2	0.0	1.7	1.5	0.6	0.3	0.0	0.0	1.5	0.7	0.8	
Story drift, $\Delta/H$ (%)																
$KL/r$	$R=1$			$R=2$			$R=4$			$R=6$			$R=8$			
50	0.23			0.60			1.36			1.42			1.56			
100	0.17			0.39			0.85			1.23			1.81			
150	0.08			0.17			0.43			0.73			0.90			
Ductility demand, $\mu = \delta_{\max}/\delta_y$																
$KL/r$	$R=1$			$R=2$			$R=4$			$R=6$			$R=8$			
50	0.66			1.71			3.88			4.06			4.46			
100	0.88			1.97			4.28			6.26			9.18			
150	0.86			1.89			4.92			8.34			10.30			

hysteretic energy ratios are related to  $KL/r$  and  $R$  values. Ductile design procedures for CBF and case studies will be discussed in the following section. Calculation sheets also with design outcomes, used for parametric and case studies, are provided in the technical report by Lee and Bruneau (2002).

The energy dissipation of bracing members in compression from experimental data was collected and reviewed by Lee and Bruneau (2002). In this study, to facilitate comparison between results from various experiments, all results were expressed in a normalized manner. The normalized compressive energy,  $E_C/E_T$ , was obtained by dividing the compressive energy,  $E_C$ , by the corresponding tensile energy,  $E_T$ , defined as the energy that would have been dissipated by the member in tension if the same maximum axial displacement,  $\delta_c$ , was reached during unloading of the member after its elongation, as illustrated in Fig. 6 (Lee and Bruneau 2002). The normalized energy dissipation was then cumulated until fracture of each bracing member. The normalized cumulative energy ( $\Sigma E_C/E_T$ ) from experimental data (Lee and Bruneau 2002) and results of analyses are summarized in Tables 3 and 4, respectively and graphically shown in Fig. 7. The cumulative energy from analyses of cases having small  $R$  values and large  $KL/r$  could not be calculated because the bracing members remained in the elastic range, defined as zone OA and AB in Fig. 4. The range of normalized cumulative energy for  $KL/r = 50$  obtained from the experimental data is contained within the shaded area in Fig. 7 (a single experimental data point in the case of  $KL/r = 150$ ). As shown in Fig. 7, as  $R$  increases, the normalized cumulative energy decreases. It is also observed that all the analysis results obtained are within the range of experimental data available. At first, this may appear to be counterintuitive, as it is generally expected that a structure

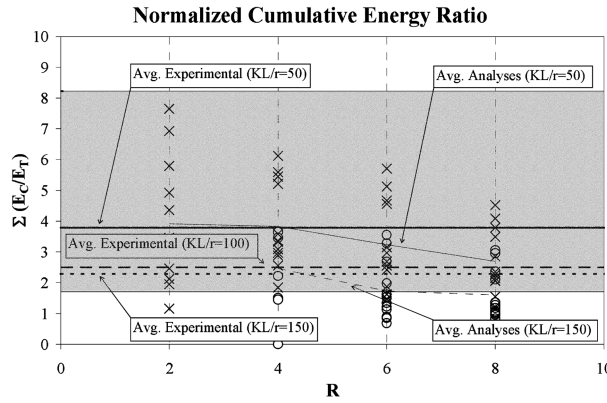


Fig. 7 Normalized cumulative energy (X :  $KL/r = 50$ , O :  $KL/r = 150$ )

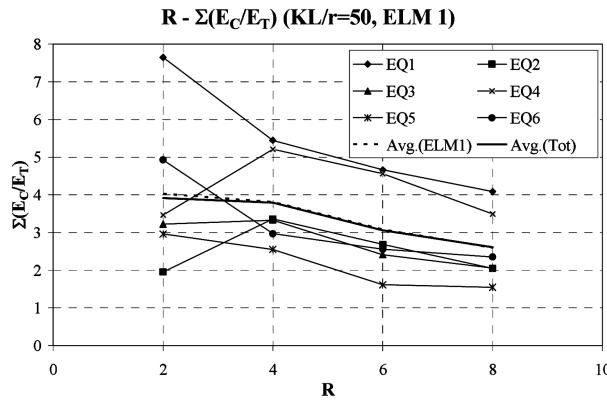


Fig. 8  $\Sigma(E_C/E_T)$  for a brace in X braced frames with  $KL/r = 50$  (Member 1)

designed with a bigger  $R$  value will have a greater ductility demand (as shown in Table 4), resulting in more energy dissipation because of this larger deformation demand. However, this can be explained as follows. The energy dissipation of a brace in compression,  $E_C$ , is obtained by calculating the area under the force-axial deformation curve, i.e., corresponding to the compression force times the axial deformation.  $E_C$  is then normalized by the corresponding tensile energy,  $E_T$ , and the sum of these values for each cycle, cumulated until the end of cyclic loading history, is defined as the normalized cumulative energy  $\Sigma(E_C/E_T)$ . This means that the normalized cumulative energy in compression is not only a function of axial deformation, but also of the compression force and tensile yield strength. The earthquake loading history also has an effect on the normalized cumulative energy in compression. Figs. 8 and 9 show the normalized cumulative energy of braces designed with same  $KL/r$  and  $R$  value, but subjected to different earthquakes. Trends are clear although exceptions occur in some cases. For example, for a  $KL/r$  value of 50 and  $R$  values increasing from 2 to 4, the normalized cumulative energy decreased when Earthquake 1 was applied, but increased when Earthquake 2 was applied. Taking Earthquake 1 as a case study that is consistent with the general trend, to illustrate the effect of  $R$  on behavior, it is first possible to observe, that although the brace designed with the larger  $R$  value of 4 deformed more than the brace designed with  $R$  of 2, the latter resists bigger forces (hysteretic curves for this example are provided in the technical report by Lee and Bruneau 2002). As the brace deforms more

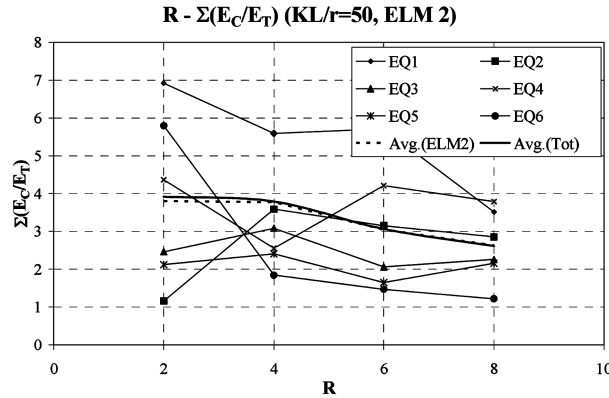


Fig. 9  $\Sigma(E_C/E_T)$  for a brace in X braced frames with  $KL/r = 50$  (Member 2)

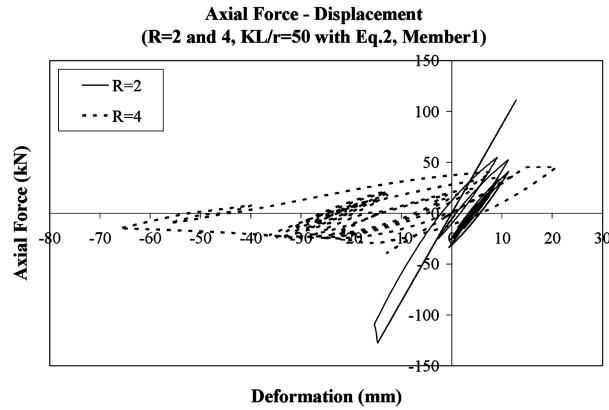


Fig. 10 Comparison of hysteretic curves for braces with  $R=2$  and  $4$ ,  $KL/r=50$

at  $R$  of  $4$ , it suffers more strength degradation which translates into a lower normalized cumulative energy. Exceptions occur when the amount of inelastic cycles for the case with greater  $R$  value overcome this effect, as shown in Fig. 10, where the bigger brace corresponding to the case with an  $R$  of  $2$  undergoes mostly cycles in the elastic range (without dissipating energy).

Fig. 7 also shows that increasing  $KL/r$  translates into a decrease in normalized cumulative energy. This means that more slender members undergo less inelastic energy demand than stocky ones, irrespectively of the  $R$  value used in design. This is a consequence of the ratio of tensile and compressive strength as a function of  $KL/r$ , which translates directly into a lower normalized energy ( $E_C/E_T$ ) for more slender members. This can be illustrated schematically using Fig. 11. In this example, the strength degradation of a brace after elastic buckling in compression is considered for all cycles except the first. The normalized energy for the 2<sup>nd</sup> and following cycles of members with  $KL/r$  of  $50$  and  $150$  are  $0.64$  and  $0.10$ , respectively, resulting in normalized cumulative energy of  $0.64n$  and  $0.10n$  respectively after  $n$  cycles. In this case, the member with  $KL/r$  of  $150$  would have to undergo roughly  $6.4$  more cycles than the member with  $KL/r$  of  $50$  to have the same resulting normalized cumulative energy. Looking at results from the analyses using actual earthquakes, a similar trend was observed. For example, as shown in Fig. 12, though the slender brace (designed with  $KL/r$  value of  $150$ ) experienced more inelastic cycle than the stocky brace (designed with  $KL/r$  value of  $50$ ), the normalized cumulative

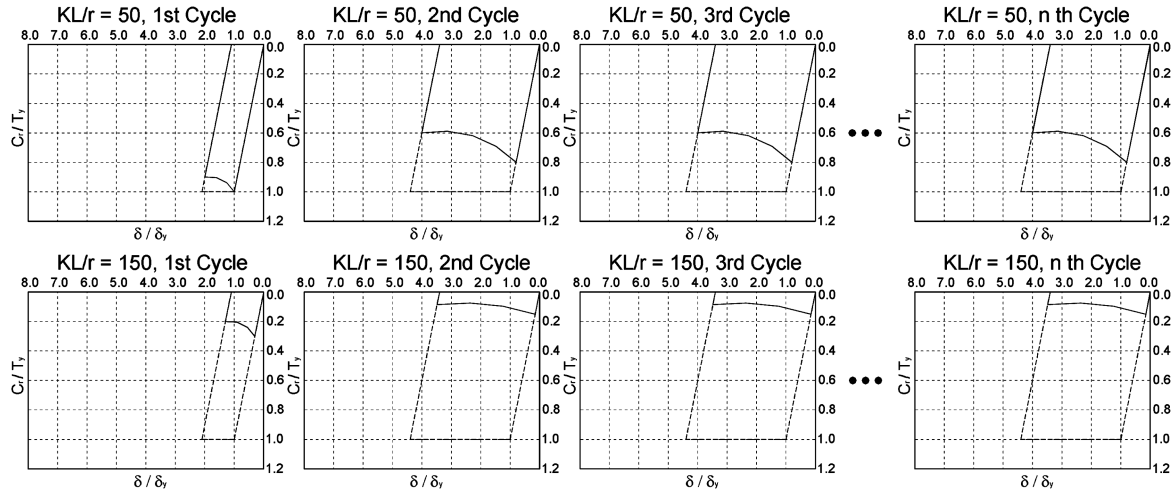


Fig. 11 Comparison the schematically normalized cumulative energy of braces with  $KL/r$  of 50 and 150

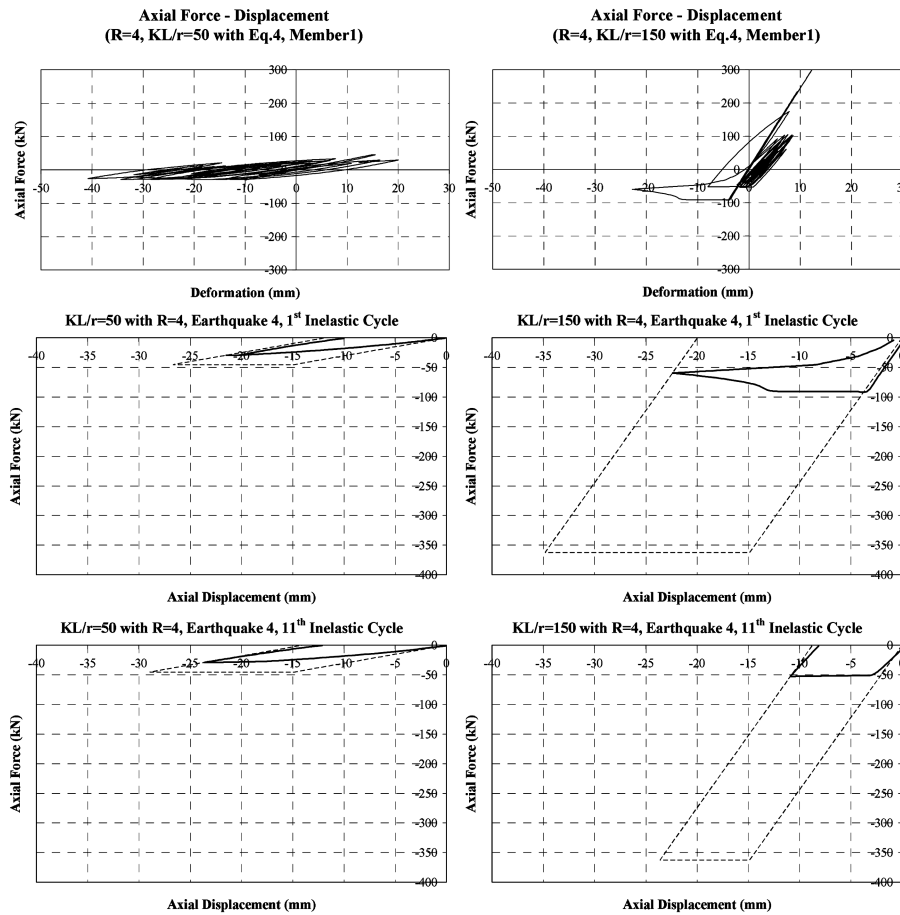


Fig. 12 Comparison of the normalized cumulative energy of braces analyzed (Braces with  $R=4$ , Earthquake 4, and  $KL/r = 50$  and 150)

Table 5 Strength design and ductile design data

$R$	Strength design			Ductile design			Code limits	
	Member(U.S.)	$KL/r$	$b/t$	Member(U.S.)	$KL/r$	$b/t$	$KL/r$	$b/t$
1	TS 7×7×1/4	122.1	26.0	TS 10×10×5/8	88.5	14.0	101.0	15.4
2	TS 6×6×1/4	143.6	22.0	TS 10×10×5/8	88.5	14.0	101.0	15.4
4	TS 5×5×3/16	171.6	24.7	TS 10×10×5/8	88.5	14.0	101.0	15.4
6	TS 5×5×1/8	169.0	38.0	TS 10×10×5/8	88.5	14.0	101.0	15.4
8	TS 4 <sup>1/2</sup> ×4 <sup>1/2</sup> ×1/8	187.9	34.0	TS 10×10×5/8	88.5	14.0	101.0	15.4

energy in compression ( $\Sigma(E_C/E_T)$ ) of the stocky brace is still bigger than for the slender brace. Here, the normalized energy ( $E_C/E_T$ ) of the stocky and slender brace in the 1<sup>st</sup> cycle (the 1<sup>st</sup> cycle with relatively large inelastic deformation) are respectively 0.39 and 0.11, and in the 11<sup>th</sup> cycle, 0.47 and 0.14, respectively. The normalized cumulative energy ( $\Sigma(E_C/E_T)$ ) are 5.22 and 3.45, respectively, even though the slender brace experienced 1.76 times more inelastic cycles.

#### 4. Parametric and case studies

##### 4.1. Redesign following AISC ductile design procedures

Bracing members were designed following ductile design procedures (AISC, 1997 and Bruneau *et al.* 1998). Ductile design starts with a strength design in accordance with the AISC LRFD Specification (AISC, 1993) and minimum weight as design objective. In that process, tubular braces were selected. Then, members obtained from strength design are evaluated and modified as necessary to guarantee ductile response of the frame, by satisfying the limits on the  $KL/r$  and  $b/t$  ratios of braces specified for SCBF (AISC, 1997). The resulting brace member sizes are summarized Table 5. Essentially, the design procedure follows the same approach as described in section 2.2, with the exception that available structural shapes are used, rather than specified section properties that may not correspond to sections currently produced. All resulting brace members are bigger than those designed following the design procedure in section 2.2. This is expected as bigger sections are typically obtained for ductile design when compared to strength design. However, because of the requirements for ductile designs, brace members ended up being the same for all cases, regardless of  $R$  values (from 1 to 6). As a result, they all behaved elastically, making all comparisons of hysteretic behavior a moot point in this case.

##### 4.2. Effects of member length, $L$ , on response modification factor, $R$

Another design approach was adopted to investigate the relationship between  $KL/r$  and response modification factor ( $R$ ), which was previously defined in Eq. (5). In this approach, for each target  $KL/r$  value, the bracing member lengths were increased while the member geometry (width, depth, and thickness) was kept constant. Design procedures otherwise followed those presented in section 2.2. Results are compared in Fig. 13. Though the tensile strengths of bracing members ( $A_g F_y$ ) remained constant in this case, the buckling strength of the bracing members ( $C_r$ ) decreased for larger  $KL/r$  values. As shown in Fig. 13,  $R$  increases for increasing values of  $L$  ( $KL/r$ ). In this context, a larger  $R$  means that structures with larger  $KL/r$  have a greater ductility demand. As seen in the previous section,

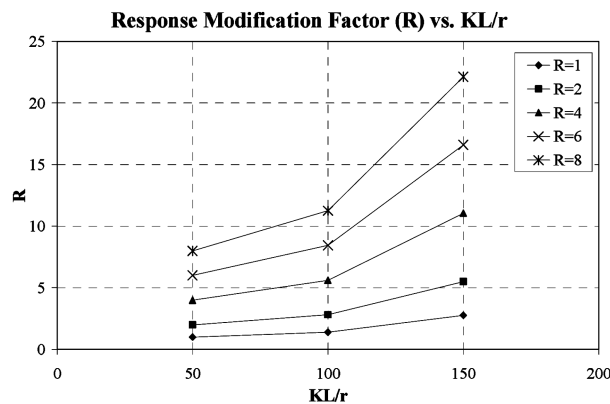


Fig. 13 Effects of member length ( $L$ ) on response modification Factor ( $R$ )

a structure with a large  $R$  value has less normalized cumulative energy dissipation. Since  $R$  increases with  $KL/r$ , this suggests that increasing  $KL/r$  in this case translate into decreasing normalized cumulative energy dissipation demand. These observations are based on the non-linear dynamic analyses reported here for  $KL/r$  of 50, 100, and 150, and the assumption that the trends can be interpolated for other values of  $KL/r$ .

## 5. Conclusions

The response of single story buildings was investigated along with a few additional case studies to outline trends in response and to develop a better understanding of the sensitivity of some design parameters on the seismic response of CBF. Results from the non-linear dynamic analyses of buildings having X-braced bay and designed using various  $R$  factors and  $KL/r$  values were correlated with results from an experimental data, database, and observations were made on how normalized cumulative hysteretic energy related to effective slenderness ratio,  $KL/r$ , and response modification factors,  $R$ .

Although a bracing member designed with bigger  $R$  value is generally expected to have larger energy dissipation by experiencing more inelastic cycles from its superior ductility demand, analysis results show that this ductile brace has less normalized cumulative energy in compression demand due to its significantly larger strength degradation after elastic buckling and its relatively smaller compressive strength.

Both analysis results and experimental data collected by Lee and Bruneau (2002) show that, in most cases, slender bracing members have higher ductility demand, but less normalized cumulative energy demand in compression.

Braces designed to satisfy more restrictive limits on  $KL/r$  and  $b/t$ , required by seismic design procedures, are often bigger than the bracing members designed following the AISC LRFD provisions. The resulting larger braces may in some cases remain elastic throughout the entire earthquake response which somehow renders the special ductile detail provisions paradoxical.

This paper provides data to either substantiate the validity or invalidity of some current perceptions regarding the effectiveness of braced frames. The paper also provides a framework for further studies to investigate the influence of  $KL/r$  and  $R$  on the seismic performance of braced frames to establish practical limits for those parameters.

## Acknowledgements

This work was conducted by the University at Buffalo and was supported by the Federal Highway Administration under contract number DTFH61-98-C-00094 to the Multidisciplinary Center for Earthquake Engineering Research. However, any opinions, findings, conclusions, and recommendations presented in this paper are those of the authors and do not necessarily reflect the views of the sponsors.

## References

- AISC (1997), "Seismic provisions for structural steel buildings", American Institute of Steel Construction, Chicago, IL.
- AISC (1993), "Load and resistance factor design specification for structural steel buildings", American Institute of Steel Construction, Chicago, IL.
- Bruneau, Michel, Uang, Chia-Ming, and Whittaker, Andrew (1998), *Ductile Design of Steel Structures*, McGraw-Hill, New York, NY.
- Gugerli, H. and Goel, S.C. (1982), "Inelastic cyclic behavior of steel bracing members", Report No. UMEE 82R1, January, Department of Civil Engineering, The University of Michigan, Ann Arbor, Michigan.
- Hassan, O.F. and Goel, S.C. (1991), "Modeling of bracing members and seismic behavior of concentrically braced steel structures", Report No. UMCE 91-1, January, Department of Civil Engineering, The University of Michigan, Ann Arbor, Michigan.
- ICBO (1994), "Uniform building code", *Int. Conf. of Building Officials*, Whittier, California
- Ikeda, K. and Mahin, S.A. (1984), "A refined physical theory model for predicting the seismic behavior of braced frames", Report No. UCB/EERC-84/12, Earthquake Engineering Research Center, University of California, Berkeley, California.
- Ikeda, K., Mahin, S.A. and Dermitzakis, S.N. (1984), "Phenomenological modeling of steel braces under cyclic loading", Report No. UCB/EERC-84/09, Earthquake Engineering Research Center, University of California, Berkeley, California.
- Jain, A.K., Goel, S.C. and Hanson, R.D. (1977), "Static and dynamic hysteresis behavior of steel tubular members with welded gusset plates", Report No. UMEE 77R3, June, Department of Civil Engineering, The University of Michigan, Ann Arbor, Michigan.
- Lee, K. and Bruneau, M. (2002), "Review of energy dissipation of compression members in concentrically braced frames", Report No. MCEER-02-0005, December, Multidisciplinary Center for Earthquake Engineering Research, University at Buffalo, Buffalo, NY.
- Lee, S. and Goel, S.C. (1987), "Seismic behavior of hollow and concrete-filled square tubular bracing members", Report No. UMEE 87-11, December, Department of Civil Engineering, The University of Michigan, Ann Arbor, Michigan.
- Nonaka, Taijiro (1987), "Formulation of inelastic bar under repeated axial and thermal loadings", *J. Eng. Mech. ASCE*, **113**(11), August, 1647-1664, Reston, Virginia.
- Prakash, V. and Powell, G.H. (1993), "DRAIN-2DX, DRAIN-3DX and DRAIN-BUILDING Base Program Design Documentation", Report No. UCB/SEMM-93/16, December, Structural Engineering Mechanics and Materials, University of California, Berkeley, California.
- Taddei, Pascal (1995), "Implementation of the refined physical theory model of braced steel frames in NONSPEC and DRAIN-2DX", August, Department of Civil Engineering, The University of Ottawa, Ottawa, Ontario, Canada.
- Tremblay, R and Lacerte, M. (2002), "Influence of the properties of bracing members on the seismic response of concentrically braced steel frames", *12<sup>th</sup> European Conf. on Earthquake Engineering*, Society for Earthquake and Civil Engineering Dynamics, London, UK.